Pergamon

Bioorganic & Medicinal Chemistry 7 (1999) 1413–1423

BIOORGANIC & MEDICINAL CHEMISTRY

Conformational Considerations in the Design of Dual Antagonists of Platelet-Activating Factor (PAF) and Histamine

James J. Kaminski,[a,*] Nicholas I. Carruthers,[a] Shing-Chun Wong,[a] Tze-Ming Chan,[a] M. Motassim Billah,[a] S. Tozzi[a] and Andrew T. McPhail[b]

[a]*Schering-Plough Research Institute, 2015 Galloping Hill Road, K15-1, 1800, Kenilworth, NJ 07033, USA*
[b]*Department of Chemistry, Duke University, Durham, NC 27708, USA*

Received 5 October 1998; accepted 8 February 1999

Abstract—Following the discovery of the first dual antagonist of platelet-activating factor (PAF) and histamine, 1-acetyl-4-(8-chloro-5,6-dihydro-11*H*-benzo[5,6]cyclohepta[1,2-*b*]pyridin-11-ylidene)piperidine, Sch 37370, **1**, a related series of structures, exemplified by (±)-1-acetyl-4-(8-chloro-5,6-dihydro-11*H*-benzo[5,6]-cyclohepta[1,2-*b*]pyridin-11-yl)piperazine, Sch 40338, **2**, were prepared. Interestingly, the compounds exhibited a parallel structure–antiallergy activity relationship, suggesting that the two series may adopt a common conformation at the PAF receptor. Conformational analysis led to a proposal for this bioactive conformation accessible to both series. The synthesis of novel conformationally constrained analogues that might mimic the proposed bioactive conformation of these compounds, and the evaluation of their in vitro antiallergy activity form the subject matter of this report.

Introduction

The pathophysiology of allergic and inflammatory diseases such as asthma is complex and probably involves the biosynthesis and/or release of multiple mediators. These mediators may be preformed, such as histamine, which acts through specific histamine H_1-receptors. Alternatively, they can be synthesized in response to antigenic stimulation, such as the leukotrienes, (LTB_4, LTC_4, and LTD_4), the prostaglandins, thromboxane A_2 (TxA_2), and platelet-activating factor (PAF). Regardless of their genesis, the presence of these mediators elicit the physiological effects that characterize the disease, i.e. smooth muscle contraction, vasopermeability, inflammatory cell influx, edema, and mucous production. The importance of the contribution that any one of these mediators makes to clinical asthma is largely unknown. However, with the expectation that an inhibitor of more than one mediator would be clinically more effective than a selective mediator inhibitor, we reported the results of the structure–antiallergy activity relationship studies[1–4] that culminated with the identification of 1-acetyl-4-(8-chloro-5,6-dihydro-11*H*-benzo[5,6]cyclohepta-[1,2-*b*]pyridin-11-ylidene)piperidine, Sch 37370 **1**, as the first dual antagonist of PAF and histamine evaluated in clinical trials.[5,6]

Following the disclosure of (**1**), we described a related, yet structurally distinct, series of compounds exemplified by (±)-1-acetyl-4-(8-chloro-5,6-dihydro-11*H*-benzo-[5,6]cyclohepta[1,2-*b*]pyridin-11-yl)piperazine, Sch 40338 (**2**) which also exhibited in vitro dual PAF and histamine H_1-receptor antagonist activity (Table 1).[7,8] This series of compounds contains a piperazine ring attached to the 11-position of the tricyclic system in place of the piperidinylidene ring.

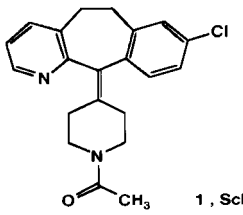

1, Sch 37370

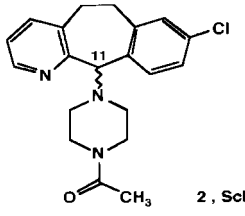

2, Sch 40338

Replacement of the Δ^{11}-carbon-to-carbon double bond with a carbon-to-nitrogen single bond, in addition to introducing a chiral center at C-11 in the molecule, also significantly increases the conformational space accessible to analogues in the piperazine series relative to those in the piperidinylidene class.

Key words: Platelet activating factor (PAF); H_1-receptor antagonist; conformational analysis; rigid analogues; molecular modeling.
* Corresponding author. Tel.: +1-908-740-3521; fax: +1-908-740-7545; e-mail: james.kaminski@spcorp.com

0968-0896/99/$ - see front matter
PII: S0968-0896(99)00075-9

More recently, we have extended our investigations to include (±)-1-acetyl-4-(8-chloro-5,6-dihydro-11*H*-benzo[5,6]cyclohepta[1,2-*b*]pyridin-11-yl)piperidine (**3**) and (±)-1-acetyl-4-(8-chloro-5,6-dihydro-11-methyl-11*H*-benzo[5,6]cyclohepta[1,2-*b*]-pyridin-11-yl)piperidine **4**

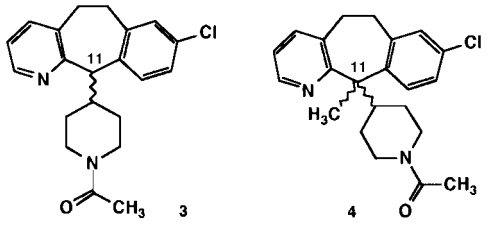

In these two classes of compounds, a piperidine ring is attached to the 11-position of the tricyclic system in place of either the piperazine or piperidinylidene rings. Furthermore, in **4**, the C-11 hydrogen atom in **2** has been replaced by a methyl group, the presence of which introduces additional *gauche* interactions with the piperidine ring, thereby, affecting even further the conformational space accessible to analogues of this series. Interestingly, while **3** and **4** exhibit differing levels of PAF antagonist activity relative to either **1** or **2**, both compounds are essentially devoid of histamine H_1-receptor antagonist potency (Table 1). These limited observations led us to propose the existence of an interrelationship between the conformational requirements of these compounds and their antiallergy activity. Conformational analysis of **1–4**, examined using a variety of theoretical and experimental methods, suggested a bioactive conformation for these series. Synthesis of rigid analogues that might mimic the proposed bioactive conformation of these compounds, and evaluation of their in vitro antiallergy activity form the subject matter of this report.

Chemistry

Synthesis of the desired rigid analogues proceeded from the tricycle **16** which was obtained from ketone **14**[9,10] (Scheme 1). Thus, **14** was reduced to alcohol **15**, and the hydroxyl group was removed via conversion to the corresponding chloride followed by treatment with zinc and acetic acid. Tricycle **16** was condensed with methyl 1,2,5,6-tetrahydro-1-methylnicotinate **17** to afford the Michael addition product **18**. Condensation of **16** with **17** proceeded in satisfactory yield only when the anion of **16** was generated with sodium amide in ammoniacal dimethoxyethane, with the ammonia being removed by distillation prior to the addition of **17**. Hydrolysis of **18** to its corresponding carboxylic acid was followed by

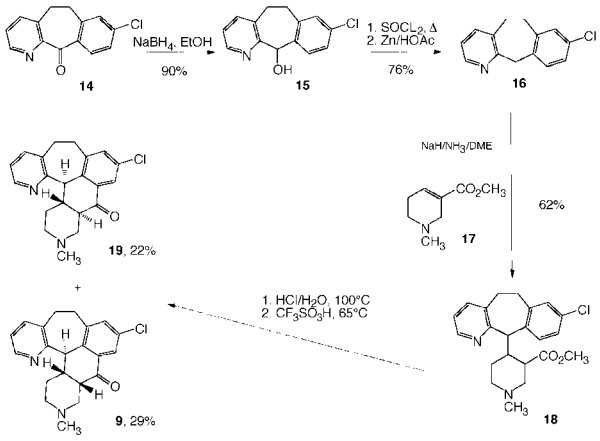

Scheme 1. Synthesis of (±)-3-methyl-7-chloro-2,3,4-b,4a,9,10,14b-α,14c-β octahydropyrido(3″,2″:6′.7′)cycloheptа(1′,2′,3′:4,5)naphtho (2,3-*c*)pyridin-5(1*H*)-one, **9**, and (±)-3-methyl-7-chloro-2,3,4,4a-α,9,10,14b-α,14c-β octahydropyrido(3″,2″:6′.7′)cycloheptа(1′,2′,3′:4,5) naphtho(2,3-*c*)pyridin-5(1*H*)-one **(19).**

Table 1. In vitro antiallergy activity and Macromodel MM2 conformational energies of **1** and related analogues

Compd	PAF antagonist[a] IC_{50} (μM)	H_1-binding[b] K_i (μM)	pA_2[c]	$E_{equatorial}$ (kcal/mol)	E_{axial} (kcal/mol)	$\Delta E_{axial->equatorial}$ (kcal/mol)
1	0.61 ± 0.05[d]	0.32 ± 0.09[e]				
2	0.59 ± 0.05[d]	5.4 ± 0.5[e]		+29.9	+26.3	−3.6[f]
3	2.5[g]	—[h]		+31.2	+26.2	−5.0
4	> 50g	—[i]		+40.6	+35.5	−5.1
5	> 50[g]	0.05[g]	7.30			
7	3000[g]					−4.8[j]
8	300[g]					
10	3.7[g]					
11	14.3[g]			+33.3	+32.3	−1.0
12	> 50[g]	0.00017[g]	9.76			
13		0.001[g]	8.85			

[a] Values are a measure of the concentration of the drug required to cause a 50% inhibition of PAF-induced platelet aggregation of human platelet-rich plasma when challenged with 25 nM PAF.[1] The values represent the mean of two independent experiments unless otherwise indicated.

[b] Values were determined using a receptor binding assay using rat brain membranes and the experimentally determined value of 2.7 nM for the K_D of [^{3}H] pyrilamine.[1]

[c] $pA_2 = -\log$ [B], where [B] is the dose of antagonist that necessitates doubling the dose of agonist to compensate for the action of the antagonist.

[d] Value is the mean ± the standard error of the mean for eleven independent experiments.

[e] Value is the mean ± the standard error of the mean for eight independent experiments.

[f] Protonated form of **2**: $E_{equatorial} = +31.3$ kcal/mol and $E_{axial} = +29.9$ kcal/mol, $\Delta E_{axial->equatorial} = -1.4$ kcal/mol.

[g] Approximate value of IC_{50} or K_i, correlation coefficient (r^2) for the analysis > 0.9.

[h] Binding to histamine-H_1 receptor: 32% inhibition at 2.8 μM.

[i] Binding to histamine-H_1 receptor: 0% inhibition at 2.8 μM.

[j] Global minimum energy conformation, $E = +27.8$ kcal/mol. Local minimum conformation, $E = +32.6$ kcal/mol.

Friedel–Crafts acylation to afford the pentacyclic ketones **9** and **19**. Although **9** and **19** were separable, it was more convenient to complete the synthesis using the mixture since the differing chiral center was removed and regenerated in the subsequent steps (Scheme 2). The *N*-methyl piperidines **9** and **19** were transformed to their *N*-acetylpiperidines **21** via their corresponding carbamates **20**. Direct removal of the ketone carbonyl group in **21** was unsuccessful using a variety of experimental conditions. Furthermore, when the ketone carbonyl group in **21** was reduced to produce alcohol **22**, direct removal of the hydroxyl group in **22** was also unsuccessful using a variety of experimental conditions. Therefore, **22** was dehydrated using trifluoromethanesulfonic acid to produce olefin **23**. Catalytic hydrogenation of **23** produced a mixture of the desired pentacyclic targets **7** and **8**.

To investigate the effect of steric bulk at the C-10 position of the analogue on the biological activity required the synthesis of **10** and **11**. Synthesis of **10** proceeded from ketone **24** (Scheme 3). Treatment of **24** with *N*-methylpiperidine-4-magnesium chloride followed by dehydration of the addition product produced **25**. Conversion of **25** to **10** was accomplished using the procedures that were used to convert **9** and **19** to **21**. Analogues **3** and **11** were prepared from nitrile **26** (Scheme 4). Treatment of **26** with *N*-methylpiperidine-4-magnesium chloride gave intermediate ketone **27**. Sodium borohydride reduction of **27** produced the alcohol **28**. Cyclization of **28** using polyphosphoric acid produced the required ring systems, albeit in low yield. The 8-chloro and 10-chloro isomers, **30** and **29**, respectively, were separated and transformed into **3** and **11** via their corresponding carbamates as described previously.

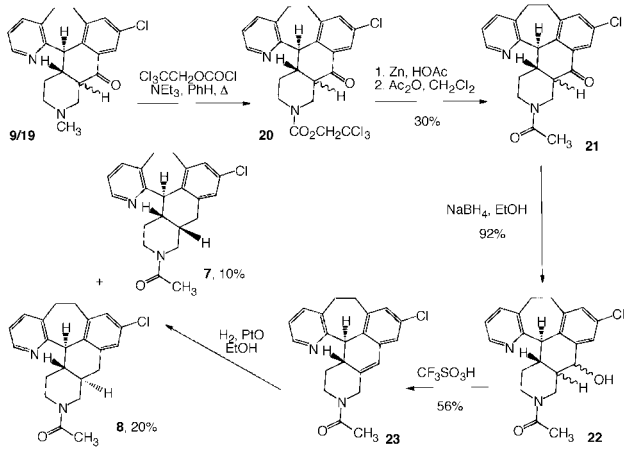

Scheme 2. Synthesis of (±)-3-acetyl-7-chloro-1,2,3,4,4a-β,5,9,10,14b-α,14c-β decahydropyrido(3″,2″:6′,7′)-cyclohepta(1′,2′,3′:4,5)naphtho-(2,3-*c*)pyridine (**7**) and (±)-3-acetyl-7-chloro-1,2,3,4,4a-α,5,9,10,14b-α,14c-β decahydropyrido(3″,2″:6′,7′)cyclohepta(1′,2′,3′:4,5)naphtho(2,3-*c*)pyridine (**8**).

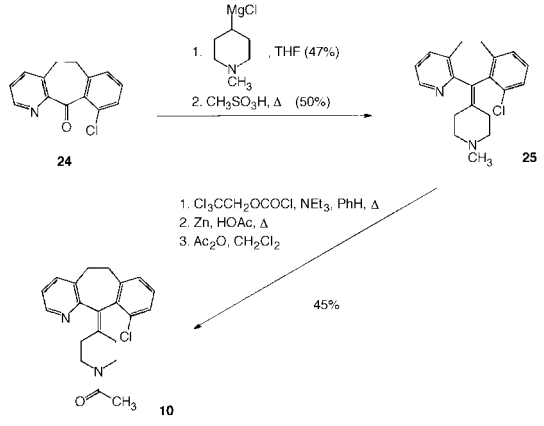

Scheme 3. Synthesis of 1-acetyl-4-(10-chloro-5,6-dihydro-11*H*-benzo[5,6]cyclohepta[1,2-*b*]pyridin-11-ylidene)piperidine (**10**).

Biological test methods

Platelet aggregation assay. Inhibition of PAF-induced aggregation of human platelets was determined using the experimental protocol described by Billah et al.[1]

Histamine-H_1 binding assay. The assay was performed using the experimental protocol described by Billah et al.[1]

Computational methods

Calculations were performed with SYBYL Version 5.3 and MacroModel V2.7 using a Silicon Graphics Challenge XL operating under IRIX.

Results and Discussion

Conformational analysis

A conformational search of **1** using a combination of SYBYL Version 5.3 and MacroModel V2.7 suggested four conformational states for the ring system (Fig. 1). In addition, three distinct conformations of **1** within ca. 5 kcal/mol of its global minimum energy conformation were also identified (Fig. 2). The difference in energies (ΔE) observed between the conformations that result from interconversion of the central seven-membered ring of the

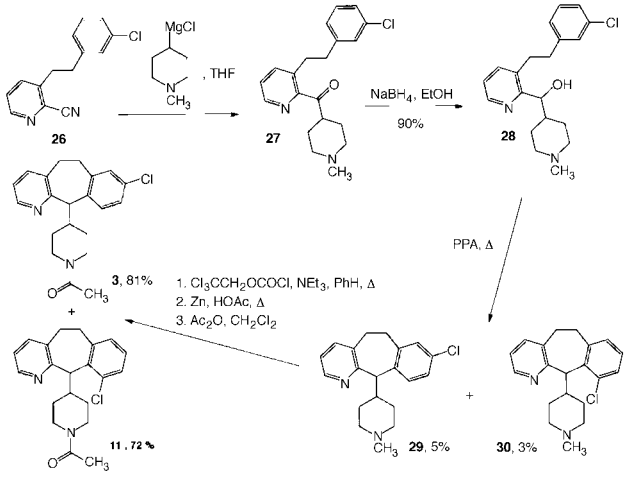

Scheme 4. Synthesis of (±)-1-acetyl-4-(8-chloro-5,6-dihydro-11*H*-benzo[5,6]cyclohepta[1,2-*b*]pyridin-11-yl)piperidine (**3**) and (±)-1-acetyl-4-(10-chloro-5,6-dihydro-11*H*-benzo[5,6]cyclohepta[1,2-*b*]pyridin-11-yl)piperidine (**11**).

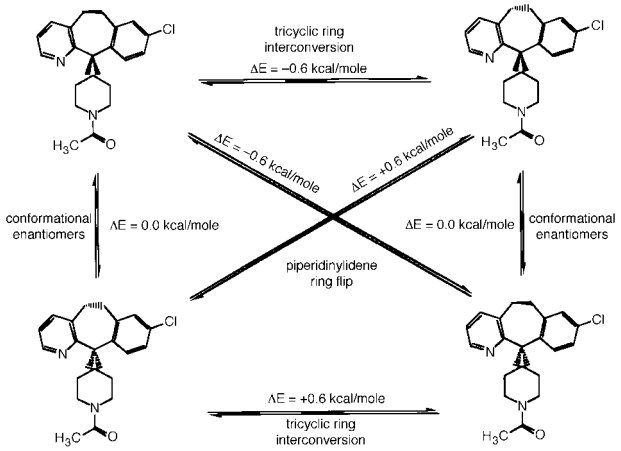

Figure 1. Conformational analysis of 1-acetyl-4-(8-chloro-5,6-dihydro-11*H*-benzo[5,6]cyclohepta[1,2-*b*]pyridin-11-ylidene)piperidine (**1**).

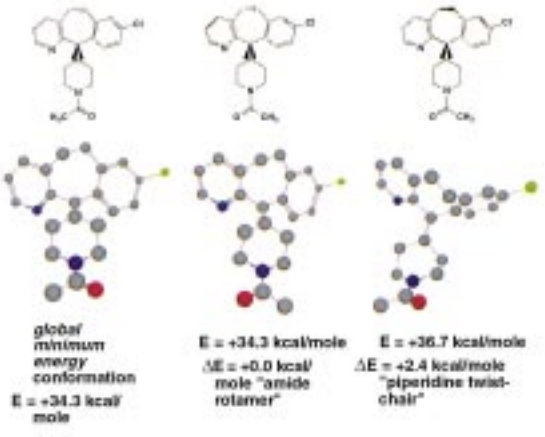

Figure 2. Conformations accessible to 1-acetyl-4-(8-chloro-5,6-dihydro-11*H*-benzo[5,6]cyclohepta[1,2-*b*]pyridin-11-ylidene)piperidine (**1**) within 5 kcal/mol of its global minimum energy conformation.

tricyclic system are equal and opposite to the differences in energies (ΔE) observed between conformations that result from different orientations of the piperidinylidene ring with respect to the central seven-membered ring of the tricyclic system, i.e. $\Delta E = \pm 0.6$ kcal/mol. As a result, the four conformational states accessible to the ring system are in dynamic equilibrium and atropisomers are not observed at ambient temperature.

However, while conformations of **1** that differ only in the orientation of the amide carbonyl are isoenergetic, the rotational barrier of the amide was sufficiently high relative to the ^{1}H NMR time scale such that distinct resonances corresponding to each rotameric form of the amide were observed. Another higher energy conformer of **1**, but within 5 kcal/mol of the global minimum, has the piperidine ring in a twist-chair conformation (Fig. 2).

The global minimum energy conformation of **1** was compared to the solid-state conformation of loratadine, **5**, determined by single-crystal X-ray analysis (Fig. 3. The conformations were compared by fitting the atoms of the tricyclic ring system by use of the "FIT" command in SYBYL 5.3. Interestingly, the global minimum energy conformation of **1** determined in the gas phase differs from the solid-state conformation of **5** only in the conformation of the central seven-membered ring of the tricyclic system, i.e. the energy difference between twist orientation conformers of **1** differs by 0.6 kcal/mol (Fig. 1). The weighted root mean square deviation for the fit is RMS = +0.4006 Å.

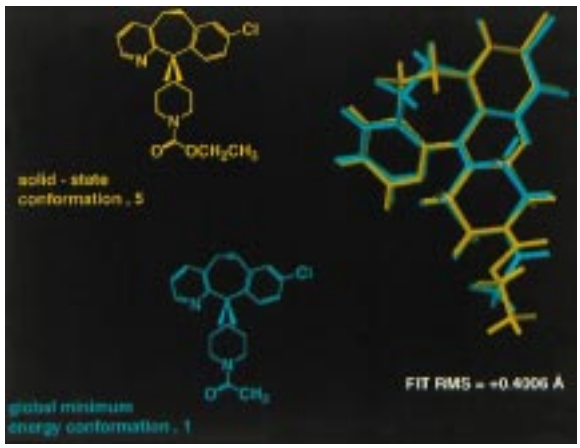

Figure 3. Comparison between the global minimum energy conformation of **1** and the solid-state conformation of loratadine, (**5**).

Conformational searches and determination of the global minimum energy conformations for **2**, **3**, and **4** were also investigated; the results are summarized in Table 1. These analogues contain either a piperazine or piperidine ring attached to the 11-position of the tricyclic system in place of the piperidinylidene ring. Replacement of the Δ^{11}-carbon-to-carbon double bond with a carbon-to-nitrogen single bond in these analogues allows the heterocycle attached to C-11 to occupy either an axial, or an equatorial position with respect to the conformation of the central seven-membered ring of the tricyclic system. Comparison between the MacroModel MM2 energies of the axial and equatorial conformers of **2**, **3**, and **4** suggests that in each case, the heterocyclic substituent at the 11-position prefers to be axially oriented in its global minimum energy conformation (Table 1).

Recently, the single-crystal X-ray structure of the (−)-isomer of **2**, as its *N*-acetyl D-leucine salt, has been determined and its absolute configuration has been established as the *S*-stereoisomer, **2**.[7,8]

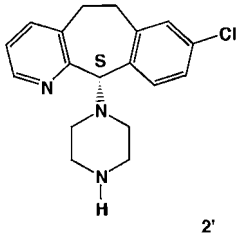

2′

In the solid-state, the piperazine ring of **2′** prefers to adopt an axial orientation. In solution, an axial orientation for the piperidine ring in **3** has also been established with the observation of a positive nuclear

Overhauser enhancement (NOE) between H_{11} and the aromatic proton attached to C-10 in its ^1H NMR spectrum. These observations are consistent with the preferred axial orientation of the piperazine and piperidine rings predicted from the global minimum energy conformations of **2**, **3**, and **4**, determined in the gas phase. Furthermore, they are consistent with the results of conformational studies described for similar systems.[12]

The in vitro potencies for PAF antagonism of **1** and **2** are identical (Table 1). In addition, the structure–anti-allergy activity relationship studies for the two series parallel each other closely.[7,8] These observations suggest that both compounds may bind to the PAF receptor in a similar manner, and the two compounds may share a common bioactive conformation. While conformational analyses of **1** and **2** suggest that their global minimum energy conformations are quite different (Fig. 4a), a common conformation is accessible in which the conformation of **2** is only slightly higher in energy, 3.6 kcal/mol (Table 1). It should be noted that the pK_a of the basic piperazine nitrogen atom in **2** is such that at physiologic pH 7.4 it will predominantly exist in its protonated form. Under these circumstances, the axial orientation of the piperazine ring is still preferred relative to its equatorial orientation, however, the difference in energy (ΔE) between these two conformations is lower, 1.4 kcal/mol (Table 1). Regardless of the state of protonation of the piperazine nitrogen atom, the conformation in which the piperazine ring is equatorial with respect to the central seven-membered ring of the tricyclic system may represent the bioactive conformation at the PAF receptor (Fig. 4b). In order for **3** and **4** to mimic the proposed bioactive conformation of **1**, their axially oriented C-11 substituent must also occupy an equatorially oriented position. Thus, we proposed that for each analogue, the magnitude of the difference in energy (ΔE) associated with orienting the C-11 substituent equatorially from its preferred axial global minimum energy orientation, should be reflected in the in vitro potency observed for PAF antagonism of the corresponding analogue, i.e., the greater the $\Delta E_{\text{axial-> equatorial}}$, the lower the in vitro potency for PAF antagonism of the analogue. The trend observed between the in vitro potency for PAF antagonism and the energetic cost associated with the axial-to-equatorial conformational change of the C-11 substituent of each analogue described in the Table 1 is consistent with this prediction. This observation prompted the design and synthesis of conformationally constrained analogues that might mimic the proposed bioactive conformation of **1**.

Synthesis of rigid analogues that might mimic the proposed bioactive conformation of 1. The pentacyclic ring system, exemplified by **6**, was designed as a potential class of compounds that might mimic the proposed bioactive conformation of **1**. Conformational rigidity imposed by the introduction of an additional six-membered ring formed by joining C-10 of the tricylic system to the β-carbon atom of the piperidine ring through an intermediate carbon atom could satisfy this requirement. However, the pentacyclic ring system proposed contains three asymmetric centers and can potentially exist as four possible diastereomeric pairs.

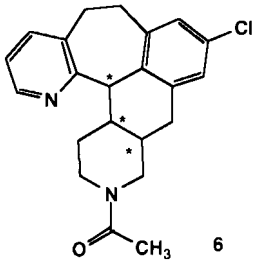

6

Synthesis of this novel ring system has been accomplished,[13] and resulted in the preparation of two diastereoisomers in racemic form, (±)-3-acetyl-7-chloro-1,2,3,4, 4a-β,5,9,10,14b-α,14c-β-decahydropyrido (3″,2″:6″,7″)cyclohepta(1′,2′,3′:4,5)-naphtho(2,3-*c*)pyridine, **7** and (±)-3-acetyl-7-chloro-1,2,3,4,4a-α,5,9,10,14b-α,14c-β-decahydropyrido(3″,2″:6″,7″)-cyclohepta(1′,2′,3′:4,5) naphtho(2,3-*c*)pyridine, **8**.

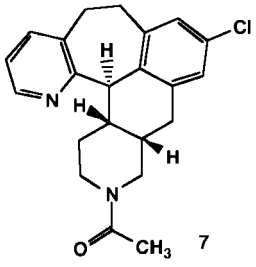

7

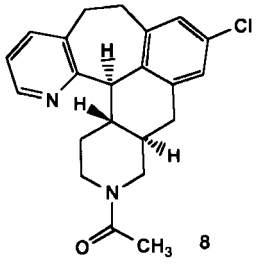

8

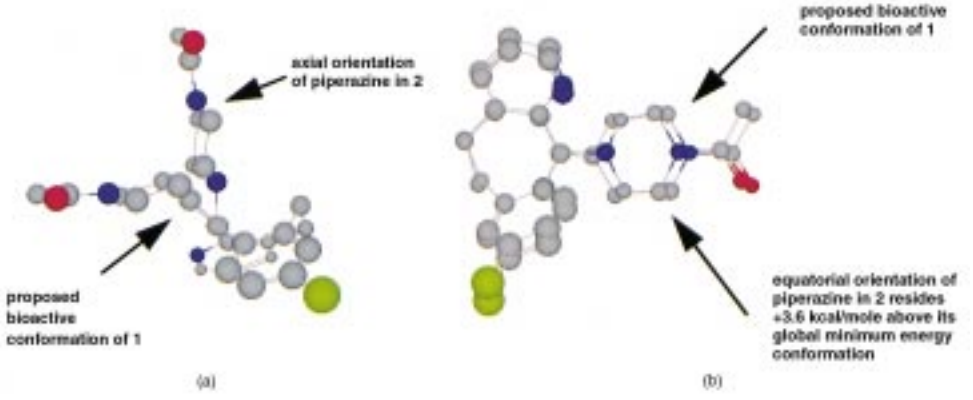

Figure 4. (a) Global minimum energy conformations of **1** and **2**. (b) A higher energy conformation of **2** that mimics the proposed bioactive conformation of **1**.

Assignment of the relative stereochemistry at the ring junctions in the two racemic diastereomeric products was established by 2-D NOESY experiments, and the 1H NMR stereochemical assignment in (±)-3-methyl-7-chloro-2,3,4-b,4a,9,10,14b-β,14c-β-octahydropyrido(3″, 2″:6′.7′)cyclohepta(1′,2′,3′:4,5) - naphtho(2,3 - *c*)pyridin - 5(1*H*)-one, **9**, an intermediate precursor to the final products, was corroborated unequivocally by single-crystal X-ray analysis (Fig. 5).

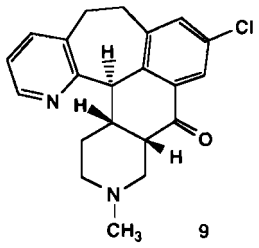

9

The gas-phase global minimum energy conformations of **7** and **8** were identified using a combination of systematic search and molecular dynamics techniques. The global minimum energy conformation of **7** determined in the gas phase is consistent with the solid-state and solution conformation of **9** determined by single-crystal X-ray analysis and ^{1}H NMR spectroscopy, respectively. Comparison between the global minimum energy conformations of **7** and **8** to the proposed bioactive conformation of **1**, suggests that **8** may better mimic the bioactive conformation relative to **7**. However, a local minimum energy conformation is accessible to **7** which is only slightly higher in energy, 4.8 kcal/mol, which better mimics the bioactive conformation of **1**, (Fig. 6a, b and c).

In either case, determination of the in vitro potencies for PAF antagonism of **7** and **8** suggested that both diastereoisomers are inactive antiPAF agents. The difference in energy associated with **7** adopting a local minimum energy conformation rather than its global minimum energy conformation to better mimic the bioactive conformation of **1** is 4.8 kcal/mol. While the magnitude of this energy difference (ΔE) might be considered sufficient to account for the inactivity of **7** as an antiPAF agent, it is inconsistent with the in vitro anti-PAF potency observed for **3**, $IC_{50} = 2.5\,\mu M$, since **3** must also expend approximately 5 kcal/mol to adopt the bioactive conformation of **1** (Table 1).

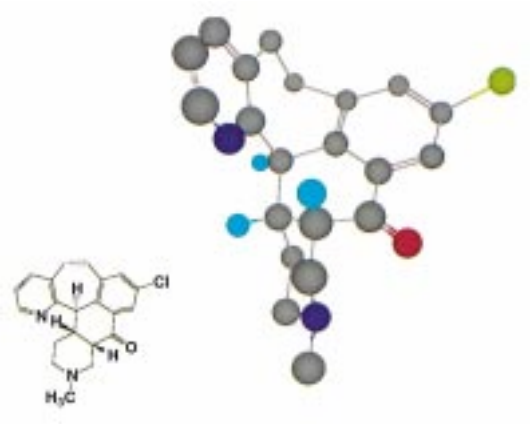

Fig. 5. Solid-state conformation of one enatiomer, (±)-3-methyl-7-chloro-2,3,4,4a-β,9,10,14b-α,14c-β octahydropyrido(3″,2″:6′.7′)-cyclohepta(1′,2′,3′:4,5)naphtho(2,3-*c*)pyridin-5(1*H*)-one (**9**), as determined by single-crystal X-ray analysis.

In the absence of further structural information regarding the binding of **7** and **8** to the PAF receptor, these observations suggest that while attainment of the proposed bioactive conformation of **1** may be a necessary condition, alone it is not sufficient to impart antiPAF activity to the analogue. On this basis, an examination of the effect of substitution at the 10-position in **1** and related analogues on their antiPAF activity was initiated.

Effect of a 10-substituent in 1 and related analogues on in vitro PAF antagonism. The magnitude of the energy difference between axial and equatorial orientations of a C-11 substituent could be markedly affected by the absence, or presence of a C-10 substituent. Comparison of the in vitro potency for PAF antagonism of **1** relative to its 10-chloro isomer, **10**, suggests that the increased steric interaction of the 10-chloro substituent decreases the antiPAF potency of the analogue by approximately sixfold, i.e. for **1**, $IC_{50} = 0.61 \pm 0.05\,\mu M$ relative to **10**, $IC_{50} = 3.7\,\mu M$. Interestingly, comparison of the in vitro potency for PAF antagonism of **3** relative to its 10-chloro isomer, **11**, suggests that the increased steric interaction of the 10-chloro substituent in this analogue also decreases the potency of the analogue by approximately sixfold, i.e. for **3**, $IC_{50} = 2.5\,\mu M$ relative to **11**, $IC_{50} = 14.3\,\mu M$. However, in the latter case, the increased steric interaction of the 10-chloro substituent in **11** concomitantly reduces the magnitude of the difference in energy (ΔE) associated with orienting the C-11 substituent equatorially from its preferred axial global minimum energy orientation relative to **3**, i.e. for **3**, $\Delta E_{\text{axial-}>\text{equatorial}} = -5$ kcal/mol relative to **11**, $\Delta E_{\text{axial-}>\text{equatorial}} = -1$ kcal/mol.

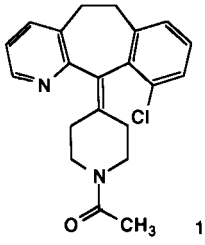

10

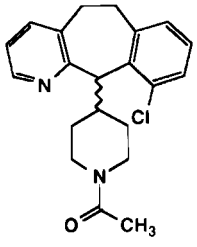

11

While the global minimum energy conformation of **8** approximates the bioactive conformation of **1**, and the energetic cost associated with **7** attaining the proposed bioactive conformation of **1** is approximately the same as that required for **3**, the in vitro potency for PAF antagonism observed for **8** and **7** are 120- and 1200-fold less, respectively, relative to the in vitro potency for PAF antagonism observed for **3**. These observations support the proposal that although the conformational constraint of the six-membered pentacyclic system in **8** and **7** may offer an entropic advantage contributing to antiPAF potency, the conformational constraint

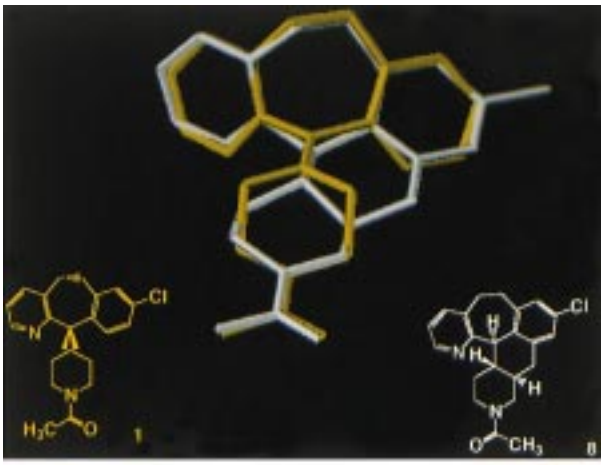

Figure 6. (a) Global minimum energy conformation of (±)-3-acetyl-7-chloro-1,2,3,4,4a-α,5,9,10,14b-α,14c-β decahydropyrido(3″,2″:6′,7′)-cyclohepta(1′,2′,3′:4,5)naphtho(2,3-*c*)pyridine (**8**) fit to the global minimum energy conformation of 1-acetyl-4-(8-chloro-5,6-dihydro-11*H*-benzo[5,6]cyclohepta[1,2-*b*]pyridin-11-ylidene)-piperidine (**1**).
(b) Global minimum energy conformation of (±)-3-acetyl-7-chloro-1,2,3,4,4a-β,5,9,10,14b-α,14c-β decahydropyrido(3″,2″:6′,7′)-cyclohepta(1′,2′,3′:4,5)naphtho(2,3-*c*)pyridine (**7**) (red) and a local minimum energy conformation of **7** (green) which resides 4.8 kcal/mol above its global minimum energy conformation fit to the global minimum energy conformation of 1-acetyl-4-(8-chloro-5,6-dihydro-11*H*-benzo[5,6]cyclohepta[1,2-*b*]pyridin-11-ylidene)-piperidine (**1**).
(c) Global minimum energy conformation of (±)-3-acetyl-7-chloro-1,2,3,4,4a-α,5,9,10,14b-α,14c-β decahydropyrido(3″,2″:6′,7′)cyclohepta (1′,2′,3′:4,5)naphtho(2,3-*c*)pyridine (**8**) and a local minimum energy conformation of (±)-3-acetyl-7-chloro-1,2,3,4,4a-β,5,9,10,14b-α,14c-β decahydropyrido(3″,2″:6′,7′)cyclohepta(1′,2′,3′:4,5)naphtho(2,3-*c*)pyridine (**7**) which resides 4.8 kcal/mol above its global minimum energy conformation fit to the global minimum energy conformation of 1-acetyl-4-(8-chloro-5,6-dihydro-11*H*-benzo[5,6]cyclohepta[1,2-*b*]pyridin-11-ylidene)piperidine (**1**).

invoked is at the expense of a significant steric interaction in an area of the PAF receptor which apparently does not tolerate steric bulk. Obviously, this conclusion is drawn in the absence of additional structural information regarding the binding of these ligands to the PAF receptor. Knowledge of this information could identify the specific interaction of the ligand with the receptor that is responsible for decreasing the antiPAF potency of the ligand.

The in vitro histamine H_1-receptor antagonist potency of (±)-7-chloro-3-methyl-1,2,3,4,4a-α,5,9,10,14b-α,14c-β - decahydropyrido(3″,2″:6′,7′) - cyclohepta(1′,2′,3′:4,5) naphtho(2,3-*c*)pyridine, **13**, was determined relative to the classical histamine H_1-receptor antagonist, *azatadine*, **12** and the nonsedating histamine H_1-receptor antagonist, *loratadine*, **5** (Table 1).

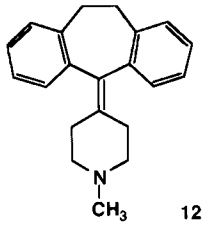

12

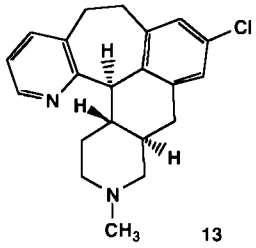

13

Comparison between either the K_i or pA_2 values suggests that **13** is a more potent H_1-receptor antagonist relative to the nonsedating antihistamine, *loratadine*, **5**, but is a weaker H_1-receptor antagonist relative to the classical antihistamine, *azatadine*, **12**. In vivo, oral administration of **13**, at a screening dose of 0.1 mg/kg, completely inhibited a histamine-induced bronchospasm in the guinea pig. However, no separation between H_1-receptor antagonist activity and sedation was observed for **13** in rats and mice.

Summary and Conclusions

In this paper, we have undertaken a conformational analysis of four series of related PAF antagonists, 1, 2, 3, and 4. These analyses suggested that the compounds might adopt a common bioactive conformation and consequently, a rigid pentacyclic ring system, **6**, was designed to mimic the bioactive conformation proposed. Two diastereoisomers, **7** and **8** were prepared and **8** was found to better approximate the bioactive conformation. However, both **7** and **8** were determined to be inactive as PAF antagonists. This result led to an evaluation of the consequences of introducing a 10-substituent, necessary for the construction of the rigid system, and thus **10** and **11** were prepared. Comparison of the in vitro potency for PAF antagonism of the 10-chloro isomers **10** and **11** with their 8-chloro analogues, **1** and **3**, respectively, suggests that the increased steric interaction of the 10-substituent is detrimental to biological activity. These results suggest that whilst the conformational constraints of the six-membered ring present in **7** and **8** may offer an entropic advantage, this is obtained only at the expense of introducing unfavorable steric bulk.

Experimental

(±)-3-Methyl-7-chloro-2,3,4-b,4a,9,10,14b-α,14c-β-octahydropyrido(3″,2″:6′.7′)cyclohepta(1′,2′,3′:4,5) naphtho(2,3-*c*)pyridin-5(1*H*)-one (9) and (±)-3-Methyl-7-chloro-2,3,4, 4a-α,9,10,14b-α,14c-β-octahydropyrido(3″,2″:6′.7′) cyclohepta(1′,2′,3′:4,5)-naphtho(2,3-*c*)pyridin-5(1*H*)-one (19). To a solution of ketone **14** (46.5 g, 190 mmol) in EtOH (400 mL) was added $NaBH_4$ (6.0 g, 160 mmol) and the mixture stirred for a further 90 min. The reaction mixture was treated with ice/H_2O (300 mL) and extracted with CH_2Cl_2 (3×200 mL). The organic portions were separated, concentrated to a slurry and redissolved in EtOAc (400 mL). This solution was washed with H_2O (2×100 mL), dried over $MgSO_4$, filtered and concentrated to a slurry. Trituration with diisopropylether afforded alcohol **15** (44.1 g). The alcohol was dissolved in benzene (500 mL) at 0 °C and treated with thionyl chloride (23.8 g, 200 mmol). The mixture was stirred at 0 °C for 15 min and at room temperature for 30 min. The solution was cooled to 0 °C and treated with 25% NaOH (250 mL), stirred for 5 min and treated with EtOAc (200 mL). The organic layer was separated, washed with H_2O (2×250 mL), dried over $MgSO_4$, filtered and evaporated to give a brown oil (~50 g). This material was dissolved in AcOH (100 mL), treated with Zn dust (12 g, 184 mmol) and heated at reflux temperature for 60 min. The reaction mixture was filtered and the residue washed with hot H_2O (3×50 mL). The combined filtrates were cooled (ice bath) and treated with excess concd NH_4OH solution. This solution was extracted with CH_2Cl_2 (3×100 mL) and the combined extracts dried over $MgSO_4$, filtered and evaporated to give a brown oil (~55 g). Trituration with diethylether afforded **16** (18.8 g) and evaporation of the supernatant followed by flash chromatography eluting with 1–5% MeOH/CH_2Cl_2 afforded additional **16** (22.6 g): Overall yield (41.4 g, 95%); mp 92–94 °C.

A solution of $NaNH_2$, prepared from Na (1.2 g, 52 mmol), NH_3 (150 mL) and $Fe(NO_3)_3 \cdot 9H_2O$ (0.05 g), was treated with a solution of **16** (11.5 g, 50 mmol) in DME (125 mL) over 15 min. A second portion of DME (125 mL) was then added and the excess NH_3 removed by warming the reaction mixture to 40 °C. The solution was then cooled to −78 °C and treated with a solution of **17** (7.75 g, 50 mmol) in DME (100 mL) over 60 min. Once the addition was complete, the cooling bath was removed and NH_4Cl (25 g) added, followed by saturated NH_4Cl solution (125 mL). This mixture was stirred for 5 min, then treated with diethylether (300 mL). The organic layer was separated and washed with H_2O (150 mL). The aqueous fractions were combined and extracted with diethylether (150 mL). The organic fractions were combined, dried over $MgSO_4$, filtered and evaporated to afford an oil (21 g). Silica gel chromatography eluting with 1.5–5.0% NEt_3/EtOAc gave **18** (12.0 g, 62%).

Ester **18** (1.3 g, 3.38 mmol) was treated with concentrated HCl (15 mL) and stirred at reflux temperature for 2 h. The reaction mixture was evaporated to dryness and the residue treated with trifluoromethanesulfonic acid (30 mL) and heated at 90–95 °C for 3 h. The solution was poured onto ice, treated with excess NH_4OH solution and

extracted with CH_2Cl_2 (3×40 mL). The organic extracts were combined, dried over $MgSO_4$, filtered and evaporated to give an oil. Silica gel chromatography eluting with 1–5% NEt_3/EtOAc gave **9** (0.35 g, 29%); mp 180–181 °C and **19** (0.27 g, 22%); mp 220–221 °C.

(±)-3-Acetyl-7-chloro-1,2,3,4,4a-β,5,9,10,14b-α,14c-β-decahydropyrido - (3″,2″:6′,7′) cyclohepta (1′, 2′, 3′: 4, 5) naphtho(2,3-*c*)pyridine (7) and (±)-3-acetyl-7-chloro-1,2, 3,4,4a-α,5,9,10,14b-α,14c-β-decahydropyrido(3″,2″:6″, 7″)cyclohepta (1′,2′,3′:4,5)naphtho(2,3-*c*)pyridine (8). A solution of **9/19** (0.27 g, 0.76 mmol) in benzene (20 mL) was treated with NEt_3 (0.3 g, 3 mmol) and trichloroethylchloroformate (0.5 g, 2.4 mmol). The mixture was heated at reflux temperature for 60 min; whereupon, a second portion of trichloroethylchloroformate (0.2 g, 0.95 mmol) was added and heating continued for an additional 30 min. The hot solution was poured onto ice and treated with excess concentrated NH_4OH solution and extracted with EtOAc (50 mL). The organic extracts were washed with H_2O (2×20 mL), dried over $MgSO_4$, filtered and evaporated to give 20 (0.36 g, 92%) mp 249–250 °C.

Carbamate **20** (0.36 g, 0.7 mmol) in AcOH (15 mL) was warmed to 60 °C to obtain a homogeneous solution, treated with Zn dust (1.2 g, 18.4 mmol) and heated at 80–90 °C for 45 min. The reaction mixture was filtered and the residue washed with H_2O (3×15 mL) and CH_2Cl_2 (2×10 mL). The filtrate was treated with excess concentrated NH_4OH solution and the organic layer separated. The aqueous portion was re-extracted with CH_2Cl_2 (2×15 mL) and the combined organic extracts dried over $MgSO_4$, filtered and evaporated to afford a waxy solid. This material was dissolved in CH_2Cl_2 (20 mL), treated with Ac_2O (1 mL, 10.6 mmol) and heated at reflux temperature for 45 min. The reaction mixture was poured onto ice, treated with excess concentrated NH_4OH solution and the organic layer separated. The aqueous portion was re-extracted with CH_2Cl_2 (3×20 mL) and the combined organic extracts dried over $MgSO_4$, filtered and evaporated to give a crude solid. Silica gel chromatography eluting with 1–8% NEt_3/EtOAc followed by recrystallization from diethylether gave **21** (0.068 g, 23%) mp 188–190 °C.

A more convenient synthesis of **21** from **18** is as follows.

Ester **18** (5.1 g, 13.25 mmol) in benzene (250 mL) was treated with NEt_3 (2.5 g, 25 mmol) followed by trichloroethylchloroformate (4.2 g, 20 mmol). The mixture was heated at reflux temperature for 60 min and then treated with additional NEt_3 (1.5 g, 15 mmol) followed by trichloroethylchloroformate (2×1 g) at 30 min intervals. After a total period of 3 h at reflux temperature, the reaction mixture was poured onto ice and treated with excess concentrated NH_4OH. The solution was extracted with diethylether (3×100 mL) and the organic extracts combined, dried over $MgSO_4$, filtered and evaporated to give a brown oil (~12 g). Silica gel chromatography eluting with 5–20% EtOAc/CH_2Cl_2 afforded the corresponding trichloroethylcarbamate (5.3 g, 74%). This material was dissolved in AcOH (25 mL), treated with Zn dust (4 g, 61 mmol) and heated at reflux temperature for 45 min. The reaction mixture was filtered and the residue washed with H_2O (3×20 mL) and CH_2Cl_2 (2×20 mL). The filtrate was treated with excess concentrated NH_4OH solution and the organic layer separated. The aqueous portion was re-extracted with CH_2Cl_2 (2×50 mL) and the combined organic fractions dried over $MgSO_4$, filtered and evaporated to approximately one-third volume. This solution was treated with Ac_2O (3 mL, 32 mmol) and heated at reflux temperature for 60 min. The reaction mixture was poured onto ice, treated with excess concentrated NH_4OH and the organic layer separated. The aqueous layer was re-extracted with CH_2Cl_2 (3×50 mL) and the combined organic fractions dried over $MgSO_4$, filtered and evaporated. Silica gel chromatography gave the corresponding acetamide (3.3 g, 85%). The acetamide was dissolved in EtOH (30 mL), treated with KOH (2.2 g, 39 mmol) and stirred at ambient temperature for 30 h. The solution was poured onto ice and adjusted to pH 5.0 by addition of concentrated HCl. This solution was extracted with CH_2Cl_2 (3×50 mL) and the extracts combined, dried over $MgSO_4$, filtered and evaporated to give a gummy solid (3.5 g). This material was dissolved in trifluoromethanesulfonic acid (30 mL) and stirred at 70–80 °C for 2 h. The solution was poured onto ice, treated with excess concentrated NH_4OH and the precipitate obtained isolated by filtration. The precipitate was dissolved in CH_2Cl_2 (150 mL), washed with H_2O (50 mL), dried over $MgSO_4$, filtered and evaporated to give a gummy solid. Trituration with diethylether gave **21** (2.8 g, 55%) mp 170–195 °C.

Ketone **21** (1.95 g, 5.1 mmol) in DME (35 mL) and EtOH (15 mL) was treated with $NaBH_4$ (0.8 g, 21 mmol) and stirred at ambient temperature for 24 h. The reaction mixture was treated with ice and extracted with CH_2Cl_2 (3×50 mL). The combined organic extracts were dried over $MgSO_4$, filtered and evaporated to give **22** (1.82 g, 92%) mp 200–210 °C.

Alcohol **22** (0.82 g, 2.14 mmol) was treated with trifluoromethanesulfonic acid (20 mL) and heated, steam bath, for 40 min. The reaction mixture was poured onto ice, treated with excess concentrated NH_4OH and the precipitate obtained isolated by filtration. The solid was redissolved in EtOAc (40 mL), washed with H_2O (10 mL), dried over $MgSO_4$, filtered and evaporated to give **23** (0.75 g, 96%).

Alkene **23** (0.5 g, 1.37 mmol in EtOH (20 mL) was treated with PtO_2 (0.03 g) and hydrogenated at 60 psi for 8 h. The reaction mixture was filtered and the filtrate evaporated to afford a foam. Silica gel chromatography eluting with 1–2% MeOH/CH_2Cl_2 gave **7** (0.05 g, 10%) and **8** (0.09 g, 20%).

1-Acetyl-4-(10-chloro-5,6-dihydro-11*H*-benzo[5,6]cyclohepta[1,2-*b*]pyridin-11-ylidene)piperidine (10). To a solution of ketone **24** (1.5 g, 6.2 mmol) in THF (50 mL) was added a THF solution (1.4 M) of *N*-methylpiperidine-4-magnesium chloride (6.0 mL, 8.4 mmol) and the reaction mixture stirred at ambient temperature overnight. The reaction mixture was treated with

saturated NH_4Cl solution (50 mL) and extracted with Et_2O (2×50 mL). The combined extracts were dried over $MgSO_4$, filtered and evaporated to afford a viscous yellow oil (2.2 g). Silica gel chromatography eluting with 2% NEt_3/EtOAc gave intermediate alcohol (1 g, 47%). The alcohol intermediate (0.9 g, 2.62 mmol) was dissolved in methanesulfonic acid (10 mL) and stirred at 100–105 °C for 24 h. The reaction mixture was poured onto ice, treated with excess concentrated NH_4OH solution and extracted with CH_2Cl_2 (3×35 mL). The organic extracts were combined, dried over $MgSO_4$, filtered and evaporated. Silica gel chromatography eluting with 1–2% NEt_3/EtOAc gave **25** (0.55 g, 65%). *N*-Methylpiperidine **25** (0.55 g, 1.7 mmol) in benzene (30 mL) was treated with NEt_3 (0.3 g, 3 mmol) and trichloroethylchloroformate (0.5 g, 2.4 mmol). The mixture was heated at reflux temperature for 2.5 h and the solution cooled by addition of ice. The solution was treated with excess concentrated NH_4OH solution and extracted with Et_2O (2×30 mL). The combined organic extracts were dried over $MgSO_4$, filtered and evaporated to afford a yellow oil (1.6 g). The crude material was purified by silica gel chromatography eluting with 2–5% NEt_3/EtOAc to afford the intermediate carbamate. The carbamate (0.44 g, 0.91 mmol) in AcOH (10 mL) was treated with Zn dust (0.4 g, 6.1 mmol) and heated at 80–90 °C for 1 h. The reaction mixture was filtered and the residue washed with hot H_2O (2×10 mL) and CH_2Cl_2 (2×20 mL). The filtrate was treated with excess concentrated NH_4OH solution and the organic layer separated. The aqueous layer was re-extracted with CH_2Cl_2 (2×20 mL) and the combined organic extracts dried over $MgSO_4$, filtered and evaporated to give a yellow oil (0.28 g). This material was dissolved in CH_2Cl_2 (20 mL), treated with Ac_2O (1 mL, 10.6 mmol) and heated at reflux temperature for 1 h. The reaction mixture was poured onto ice, treated with excess concentrated NH_4OH solution and the organic layer separated. The aqueous was re-extracted with CH_2Cl_2 (3×20 mL) and the combined organic extracts dried over $MgSO_4$, filtered and evaporated to give an oil (0.32 g). Silica gel chromatography eluting with 1–20% MeOH/CH_2Cl_2 gave **24** (0.25 g, 45%).

(±)-1-Acetyl-4-(8-chloro-5,6-dihydro-11*H*-benzo[5,6]cyclohepta[1,2-*b*]pyridin-11-yl)piperidine, (3) and (±)-1-acetyl-4-(10-chloro-5,6-dihydro-11*H*-benzo[5,6]cyclohepta[1,2-*b*]pyridin-11-yl)piperidine, (11). Ketone **27** was prepared from nitrile **26** via addition of *N*-methylpiperidine-4-magnesium chloride according to the procedure of Schumacher et al.[11] Ketone **27** (34.3 g, 100 mmol) in EtOH (400 mL) was treated, portionwise, with $NaBH_4$ (5.8 g, 153 mmol) and stirred at ambient temperature for 3 h. The solvent was evaporated under reduced pressure and the residue partitioned between CH_2Cl_2 (200 mL) and H_2O (200 mL). The organic layer was separated and the aqueous re-extracted with CH_2Cl_2 (3×75 mL). The combined organic portions were dried over $MgSO_4$, filtered and evaporated to give alcohol **28** (34 g, 99%). The alcohol was treated with polyphosphoric acid (300 g), heated at 170–175 °C for 3 h then poured onto ice (2 L). This solution was treated with excess concentrated NH_4OH solution and extracted with EtOAc (3×300 mL). The organic extracts were combined, dried over $MgSO_4$, filtered and evaporated to give a crude viscous oil (8 g). Silica gel chromatography afforded **29** (1.65 g, 5%); mp 132–134 °C and **30** (1.05 g, 3%); mp 132–139 °C.

N-Methylpiperidine **29** (1.12 g, 3.43 mmol) in benzene (20 mL) was treated with NEt_3 (0.35 g, 3.46 mmol) and trichloroethylchloroformate (1.2 g, 5.8 mmol). The mixture was heated at reflux temperature for 1.5 h and poured onto ice (50 mL). The mixture was treated with excess concentrated NH_4OH solution and extracted with EtOAc (2×20 mL). The combined organic extracts were dried over $MgSO_4$, filtered and evaporated to give an oil (2.2 g). The oil was purified by silica gel chromatography to give the intermediate carbamate (1.45 g). The carbamate in AcOH (10 mL) was treated with Zn dust (1.5 g, 23 mmol) and heated at 80–100 °C for 1 h. The reaction mixture was filtered through a glass wool plug and the residue washed with hot H_2O (2×20 mL). The combined organic extracts were dried over $MgSO_4$, filtered and evaporated to give an oil (1.2 g). This material was dissolved in CH_2Cl_2 (25 mL), treated with Ac_2O (1.5 mL, 15.9 mmol) and heated at reflux temperature for 1 h. The reaction mixture was poured onto ice, treated with excess concentrated NH_4OH solution and the organic layer separated. The aqueous was re-extracted with CH_2Cl_2 (2×25 mL) and the combined organic portions dried over $MgSO_4$, filtered and evaporated. The crude oily product was purified by silica gel chromatography eluting with 2–5% MeOH/CH_2Cl_2 to afford **3** (0.98 g, 81%). Isomeric *N*-methylpiperidine **30** (2.9 g, 8.9 mmol) was converted to **11** (1.32 g, 72%) in an analogous manner.

X-ray crystal structure analyses of compounds 2′, 5, and 9. Crystal data for **2′**: $[C_{18}H_{21}ClN_3^+][C_8H_{14}NO_3^-]$, M = 487.05, monoclinic, a = 17.740(2) Å, b = 5.783(1) Å, c = 12.886(1) Å, b = 98.05(1)°, V = 1309.0(5) Å^3, Z = 2, D_{calcd} = 1.236 g cm^{-3}, m(Cu-Ka radiation, l = 1.5418 Å) = 15.6 cm^{-1}; space group $P2_1(C_2^2)$ from the Laue symmetry and systematic absences ($0k0$ when $k \neq 2n$); crystal dimensions: 0.06×0.06×0.60 mm. Crystal data for **5**: $C_{22}H_{23}ClN_2O_2$, M = 382.89, monoclinic, a = 28.299(3) Å, b = 4.993(1) Å, c = 29.137(3) Å, b = 109.19(1)°, V = 3888(2) Å^3, Z = 8, D_{calcd} = 1.308 gcm^{-3}, m(Cu-Ka radiation) = 19.0 cm^{-1}; space group $Cc(C_s^4)$ or $C2/c(C_{2h}^6)$ from the Laue symmetry and systematic absences (hkl when $h+k \neq 2n$; $h0l$ when $l \neq 2n$), shown to be $C2/c$ by structure solution and refinement; crystal dimensions: 0.03×0.16 ×0.60 mm. Crystal data for **9**: $C_{21}H_{20}ClN_2O$, M = 351.86, triclinic, a = 10.057(1) Å, b = 10.578(1) Å, c = 9.367(1) Å, a = 111.10(1)°, b = 93.90(1)°, g = 69.95(1)° V = 871.6(3) Å^3, Z = 2, D_{calcd} = 1.341 g cm^{-3}, m(Cu-Ka radiation) = 20.3 cm^{-1}; space group $P1(C_1^1)$ or $P1(C_i^1)$ from the Laue symmetry, shown to be $P1$ by structure solution and refinement; crystal dimensions: 0.40×0.40×0.40 mm.

Oscillation and Weissenberg photographs yielded preliminary unit-cell parameters and space group information for each crystal. Intensity data ($+h, -k, \pm l$, 2972 nonequivalent reflections for **2′**; $+h, +k, \pm l$, 4062 reflections for **5**, $+h, \pm k, \pm l$, 3791 reflections for **9**) were

recorded on an Enraf–Nonius CAD-4 diffractometer [Cu-Ka radiation, graphite monochromator; w-2q scans, $q_{max} = 75°$, scanwidths $(1.15 + 0.14 \tan q)°$ for **2′**, $(1.00 + 0.14 \tan q)°$ for **5** and **9**]; the intensities of four reference reflections, remeasured every 2 h, showed no significant variation (< 1%) throughout. Refined unit-cell parameters were calculated in each case from the diffractometer setting angles for 25 reflections ($36° < q < 40°$ for **2′** and **9**; $32° < q < 36°$ for **5**) widely separated in reciprocal space. Intensity data were corrected for the usual Lorentz and polarization effects. An empirical absorption correction [T_{max}:T_{min}(relative) = 1.00:0.80], based on the f-dependency of the intensities of several reflections with c ca. 90°, was also applied to the data for **5**. Equivalent reflections for **5** and **9** were averaged [R_{merge} (on I) = 0.03 for **5**, 0.01 for **9**] to yield 3973 and 3589 nonequivalent values. The structure analyses and parameter refinements were based on 1902, 1475, and 3289 reflections with $I > 3.0s(I)$ for **2′**, **5** and **9**, respectively. All three crystal structures were solved by direct methods. For both **5** and **9**, the centrosymmetric space group choices ($P1$ and $C2/c$, respectively) were assumed at the outset and shown to be correct by the structure solutions and refinements. E-maps yielded initial coordinates for all non-hydrogen atoms in **2′** and **9**. For **2′**, the enantiomer was selected to yield the known absolute stereochemistry of the N-acetyl-D-leucyl anion. Approximate coordinates for the non-hydrogen atoms of **5**, other than those of the ethyl moiety, were obtained from an E-map; positions for the carbon atoms of the ethyl group, which was found to be disordered over two orientations, were derived from a difference Fourier synthesis phased by the other atoms. Atomic positional and thermal parameters (first isotropic and then anisotropic) were adjusted by means of full-matrix least-squares calculations during which SwD^2 $[w = 1/s^2(|F_o|), D = (|F_o| - |F_c|)]$ was minimized. Hydrogen atoms in **5** and **9** (other than those of the disordered ethyl group in **5**) were located in difference Fourier syntheses, and their positional and isotropic thermal parameters were refined in addition to the non-hydrogen atom parameters in the subsequent least-squares iterations. For **2′** and the ethyl group of **5**, hydrogen atoms were incorporated at their calculated positions. An extinction correction (g) was included as a variable during the later least-squares cycles for **2′** and **9**. The parameter refinements converged at $R(= S||F_o| - |F_c||)/S|F_o|) = 0.049$, $\{R_w = [S_w(|F_o| - |F_c|)^2/Sw(|F_o|^2]^{1/2} = 0.066$, GOF $= [SwD^2/(N_{observations} - N_{parameters})]^{1/2} = 1.28$, $g = 3.2\ (5) \times 10^{-6}\}$ for **2′**; $R = 0.044$ ($R_w = 0.055$), GOF = 1.41 for **5**, $R = 0.038$ ($R_w = 0.064$), GOF = 2.82, $g = 1.08(6) \times 10^{-5}$ for **9**. Final difference Fourier syntheses contained no unusual features [Dr(eÅ^{-3}) max, min: 0.45, −0.19 (**2**); 0.13, −0.12 (**5**), 0.30, −0.21 (**9**)].

Crystallographic calculations were performed on PDP11/44 and MicroVAX computers by use of the Enraf–Nonius Structure Determination Package (SDP). For all structure-factor calculations, neutral atom scattering factors and their anomalous dispersion corrections were taken from ref. 14.

Supplementary information available

ORTEP diagrams showing the crystallographic atom numbering schemes, tables of fractional atomic coordinates and temperature factor parameters, bond lengths, bond angles, and torsion angles for **2′**, **5** and **9** (26 pages) are available from the authors.

References

1. Billah, M. M.; Chapman, R. W.; Egan, R. W.; Gilchrest, H.; Piwinski, J. J.; Sherwood, J.; Siegel, M. I.; West, R. E., Jr.; Kreutner, W. *J. Pharmacol. Exp. Ther*. **1990**, *252*, 1090.
2. Billah, M. M.; Egan, R. W.; Ganguly, A. K.; Green, M. J.; Kreutner, W.; Piwinski, J. J.; Siegel, M. I.; Villani, F. J.; Wong, J. K. *Lipids* **1991**, *26*, 1172.
3. Piwinski, J. J.; Wong, J. K.; Green, M. J.; Ganguly, A. K.; Billah, M. M.; West, R. E., Jr.; Kreutner, W. *J. Med. Chem*. **1991**, *34*, 457.
4. Wong, J. K.; Piwinski, J. J.; Green, M. J.; Ganguly, A. K.; Anthes, J. C.; Billah, M. M. *Bioorg. Med. Chem. Lett*. **1993**, *3*, 1073.
5. Billah, M. M.; Gilchrest, H. G.; Eckel, S.; Granzow, E.; Radwanski, E.; Affrime, M.; Siegel, M. I. *J. Allergy Clin. Immunol*. **1991**, *87*, 310.
6. Berkowitz, R.; Zora, J.; Tinkelman, D.; Cuss, F.; Danzig, M.; Fourre, J. *J. Allergy Clin. Immunol*. **1991**, *87*, 167.
7. Green, M. J.; Piwinski, J. J.; Wong, J. K.; Albanese, M. A.; Colizzo, F.; Kaminski, J. J.; Ganguly, A. K.; Billah, M. M.; West, R. E., Jr.; Kreutner, W. E. Abstracts of Papers, 202nd National Meeting of the American Chemical Society; American Chemical Society: Washington, D.C. 1991; MEDI 161.
8. Piwinski, J. J.; Wong, J. K.; Green, M. J.; Kaminski, J. J.; Colizzo, F.; Albanese, M. A.; Ganguly, A. K.; Billah, M. M.; Anthes, J. C.; West, R. E., Jr. *Bioorg. Med. Chem. Lett*. **1998**, *8*, 3469.
9. Villani, F. J.; Daniels, P. J. L.; Ellis, C. A.; Mann, T. A.; Wang, K. C. *J. Med. Chem*. **1971**, *8*, 73.
10. Villani, F. J. U.S. Patent 3,326,924, 1967.
11. Schumacher, D. P.; Murphy, B. L.; Clark, J. E.; Tahbaz, P.; Mann, T. A. *J. Org. Chem*. **1989**, *54*, 2242.
12. Young, S. D.; Baldwin, J. J.; Cochran, D. W.; Kin, S. W.; Remy, D. C.; Springer, J. *J. Org. Chem*. **1985**, *50*, 339.
13. Kaminski, J. J.; Wong, S.-C.; Carruthers, N. I. U.S. Patent 5,648,360, 1997.
14. Hamilton, W. C.; Ibers, J. A., Eds. *International Tables for X-Ray Crystallography*; The Kynoch Press: Birmingham, England, 1974; Vol. IV.